$= 0 \text{ if } \Phi t > 4 \times 10^{19}$

all values in °F

Recent Guidelines

- **USNRC Reg. Guide 1.99 Rev. 2**

$$\Delta DBTT = [CF]\, f^{(0.28-0.1 \log f)} \qquad [3\text{-}5]$$

where CF is a function of Cu & Ni and a table is given in Reg. Guide 1.99, Rev. 2

- **For the new margin,**
  $\sigma_d = 28$ **for welds**
  $\sigma_d = 17$ **for base metals**

- **Note correlation with observed and calculated ΔDBTT,**
  (Figure 3-5), (Table 3-3)

USNRC Upper Shelf Toughness Requirements

- **10 CFR 50 , Appendix G specifies a minimum upper shelf Charpy impact energy requirement of 68 J (50 ft-lb)**

- **10 CFR 50 also requires that the NRC be notified 3 years in advance of the date when it is estimated that the 68 J limit will be violated**

- **At least 10 US reactors are expected to approach or violate the 68-J limit**

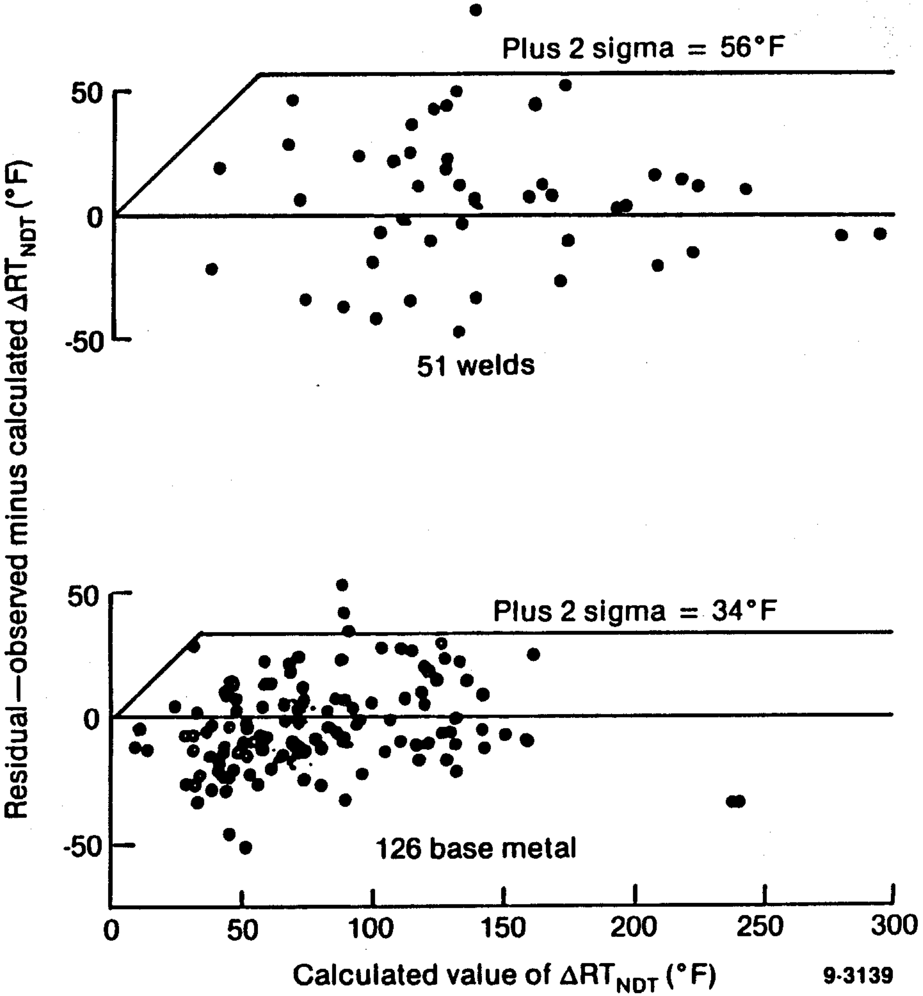

Figure 3-5. Plots of observed minus calculated versus calculated values of ΔRT_{NDT} for both welds and base metal (Randall 1986). Copyright American Society for Testing and Materials; reprinted with permission.

Table 3-3. Comparison of the two methods for calculating the final RT_{NDT}[a]

Method	Mean shift in RT_{NDT} (°F)	Initial RT_{NDT}[b] (°F)	Margin (°F)	Final RT_{NDT} (°F)
1985 PTS Rule [Equation (3-2)]	177	0	59	236
RG 1.99, Revision 2 and 1991 PTS Rule [Equation (3-5)]	235	0	66	301

---

[a] For an axial, Linde 80 weld with Cu = 0.22% and Ni = 0.77%, and a fluence of 2.5×10^{19} n/cm^2 ($E > 1$ MeV).

[b] Initial value not measured; value assumed following the PTS rule approach.

before the expiration of their current operating licenses.

Fatigue

- **Second leading cause of failure in PWR vessels**

(However, in some US plants with low-radiation-sensitive materials [i.e., Cu< 0.1 wt. % and Ni< 0.6 wt. %] and fluences < 5 x 10^{18} n/cm^2, fatigue could become the leading cause of failure)

- **Fatigue failure consists of 2 major stages:**

  a.) Crack initiation
  b.) Crack growth

- **PWR's have advantage over BWR's in *crack initiation* because of the low O_2 concentration in PWR's.**

- **Crack growth rates:**

Sub-surface cracks: $\frac{da}{dn} = \left(0.0267x10^{-3}\right)\Delta K^{3.726}\ \frac{in}{cycle}$

Surface cracks: **large ΔK's**

$$\frac{da}{dn} = \left(1.01x10^{-1}\right)(3.75R + 0.06)\Delta K^{1.95}\ \frac{in}{cycle}$$

small ΔK's

$$\frac{da}{dn} = \left(1.02x10^{-6}\right)(26.9R - 5.725)\Delta K^{5.95}\ \frac{in}{cycle}$$

where $R = \frac{K_{\min}}{K_{\max}}$

Effect of Environment

- **See figure 3-6 for the combined effects of mechanical (cycle dependent) and corrosion (time dependent) crack growth.**

Mitigation of Embrittlement Damage

- **Reduction of Thermal Stresses**

  1) Change operating procedures to eliminate off-normal events
  2) Physically change the plant design

- **Flux Reductions**

  1) Use low-leakage core loading pattern (25-50% effect)
  2) Shielding by placing steel rods or dummy fuel elements at outer edge (up to 90% effect)

- **Thermal Annealing**

  -Wet annealing (with water) at 345 °C has been accomplished in 2 reactors

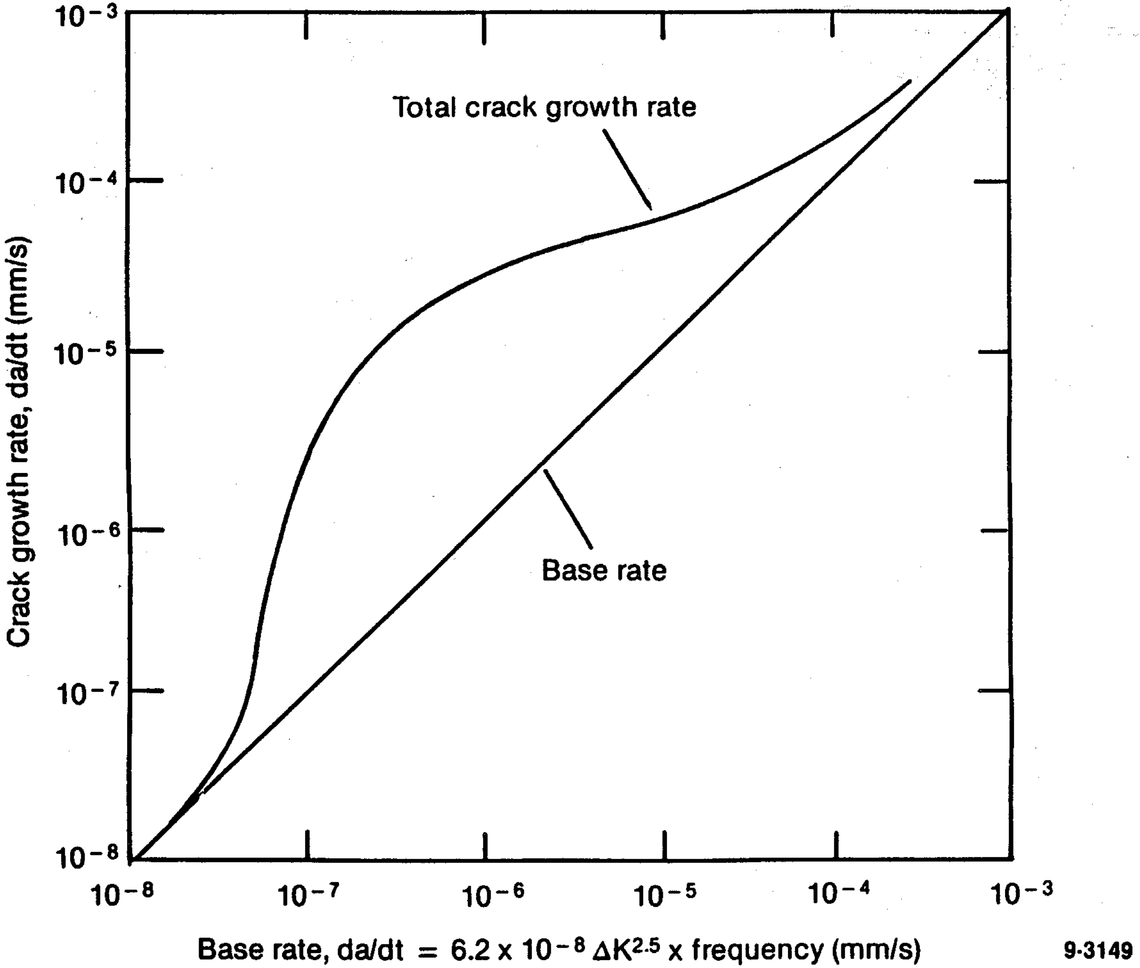

Figure 3-6. The upper bound curve showing total crack growth rate for S533B-1 steel in BWR and PWR coolant (Gilman 1987). Copyright American Society of Mechanical Engineers; reprinted with permission (modified).

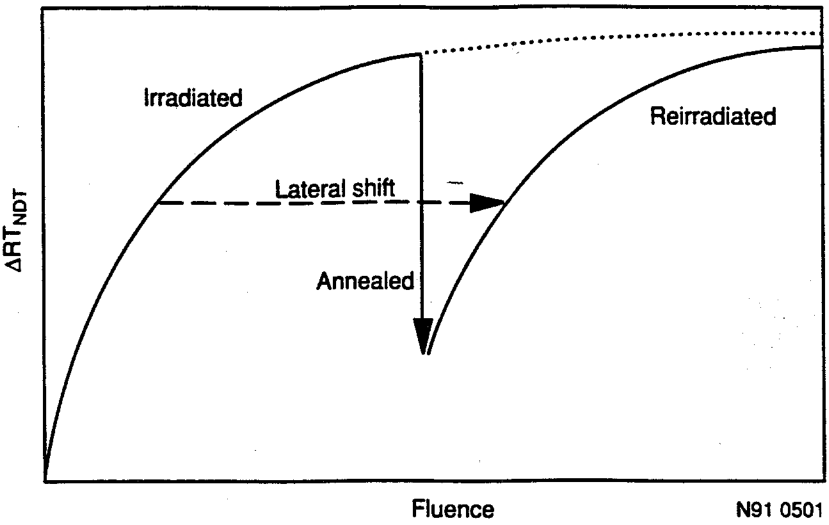

Figure 3-7. Lateral shift method for estimating reirradiation embrittlement (ASTM 1988c). Copyright American Society for Testing and Materials; reprinted with permission.

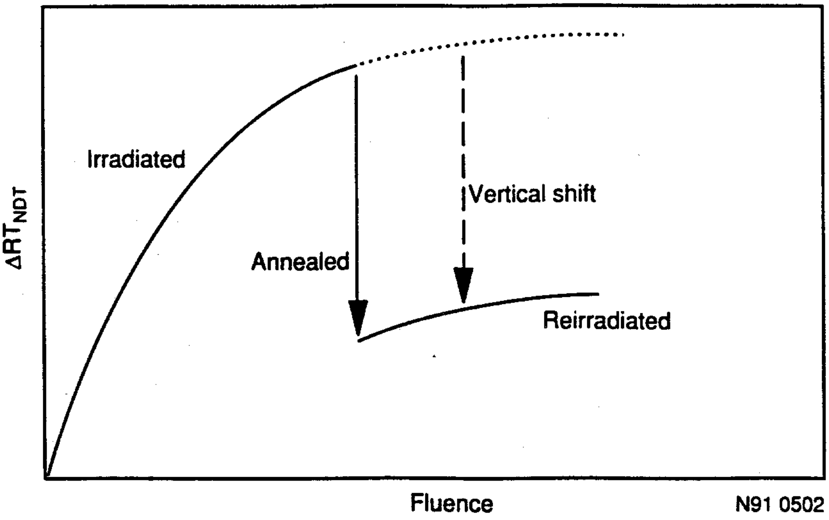

Figure 3-8. Vertical shift method for estimating reirradiation embrittlement (ASTM 1988c). Copyright American Society for Testing and Materials; reprinted with permission.

-Dry annealing (in air) @ 430 to 475 °C has been accomplished in Russian, Finnish, and US reactors

-See figure 3-8 for extent of annealing

- **Surveillance Programs**

-See figure 3-9 for location of retrievable specimens

-See figure 3-10, 3-11 for flux profiles

-Anisotropy of materials properties is addressed by taking specimens from different rolling directions (figure 3-12)

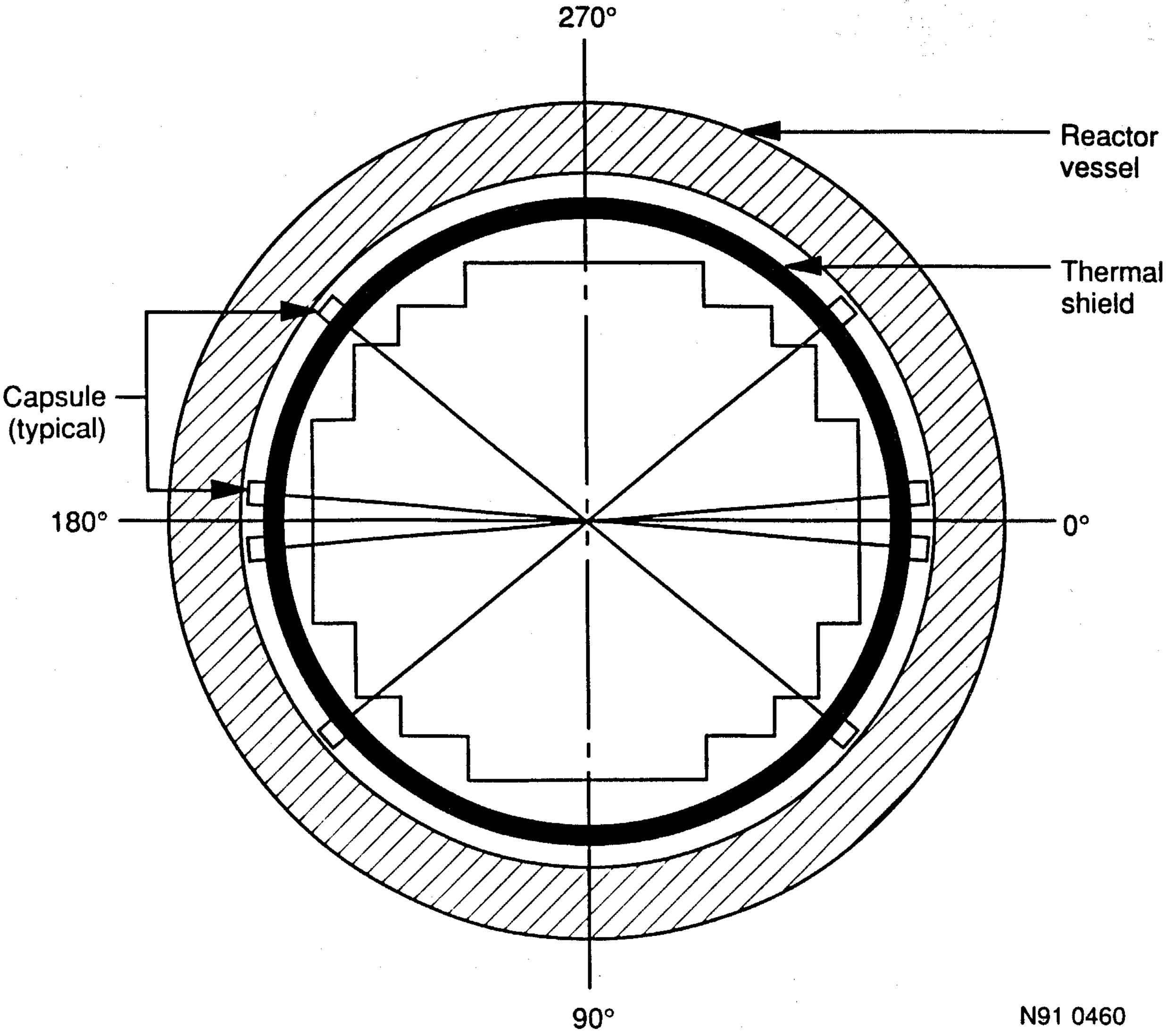

Figure 3-9. Typical locations of surveillance test capsules.

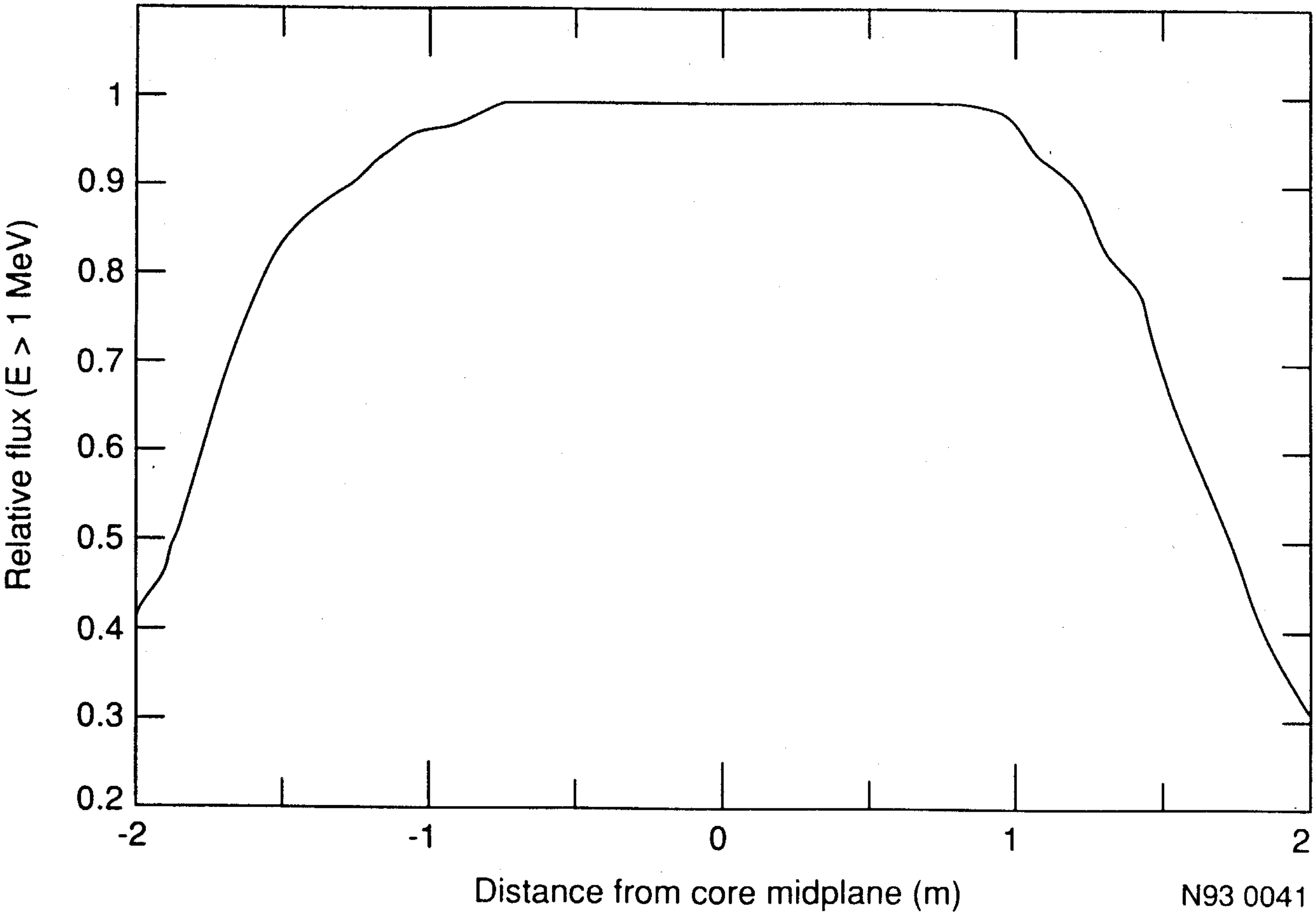

Figure 3-10. Typical axial flux distribution (relative to midcore location) at a fixed muthal location.

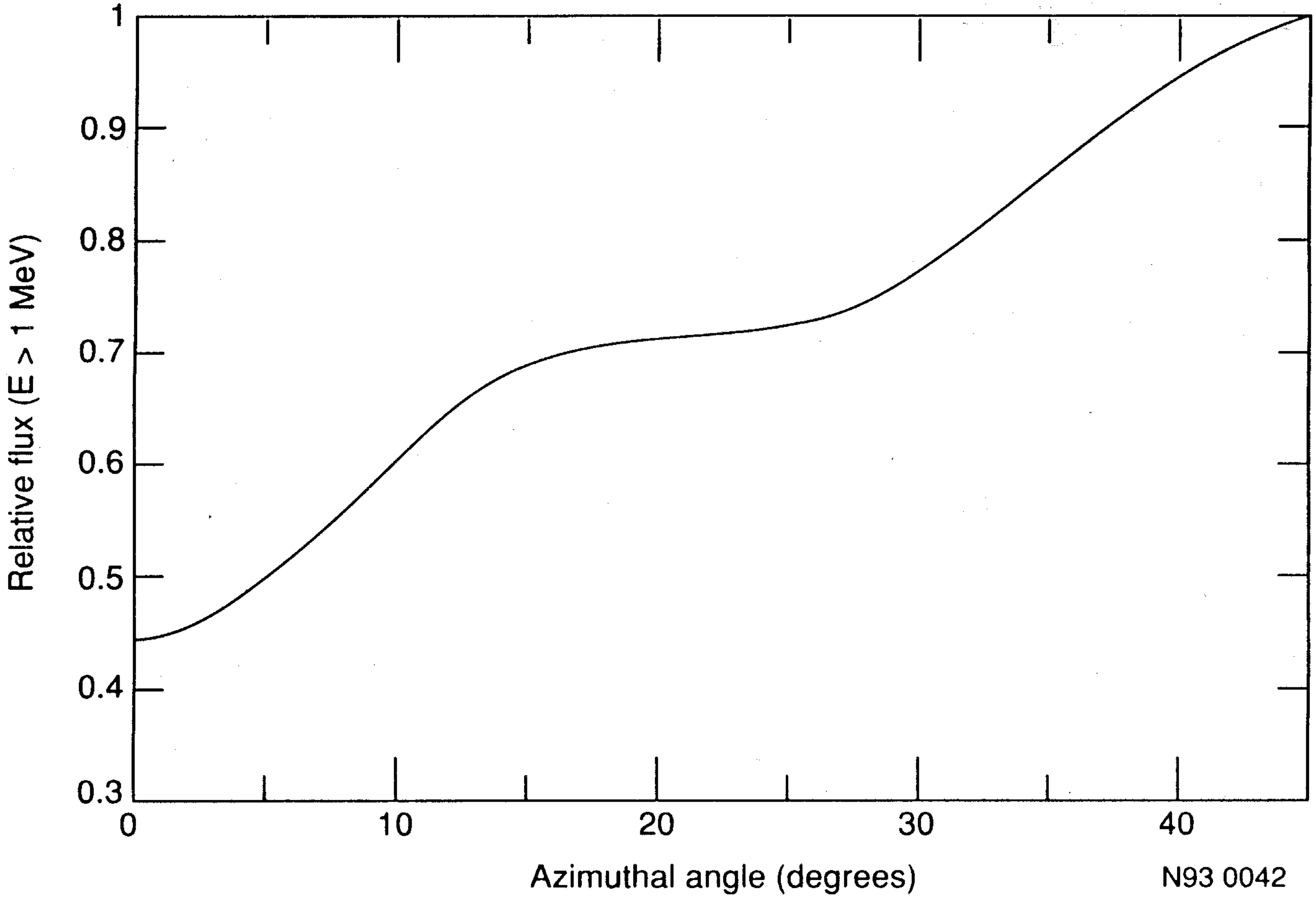

Figure 3-11. Typical azimuthal flux distribution at the core midplane. Azimuthal orientations are shown in Figure 3-9.

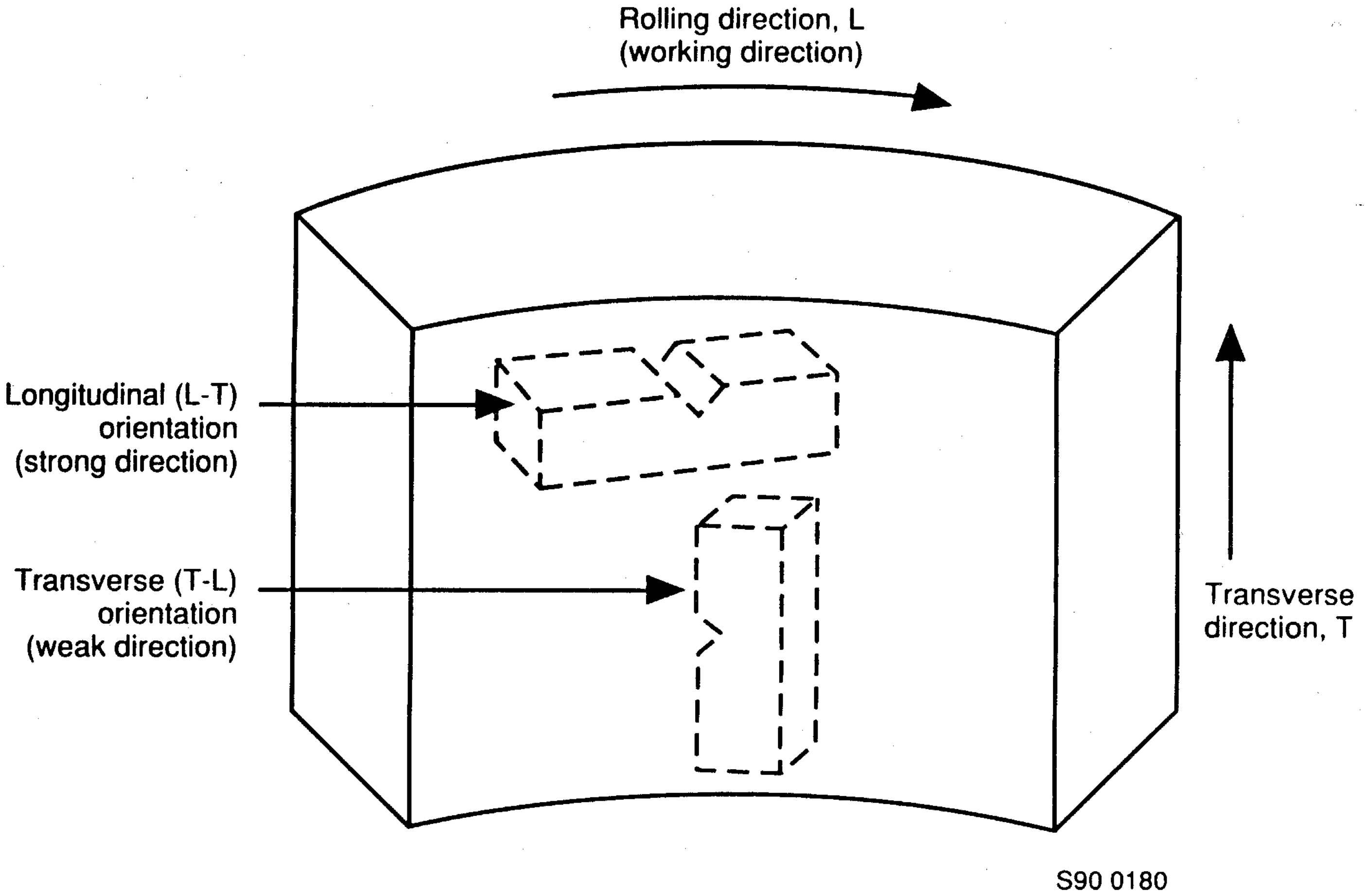

Figure 3-12. Orientations of Charpy V-notch surveillance specimens taken from vessel base material.

Boiling Water Pressure Vessels

Chapter 18 in Shah

- **Main Problems:**

  1.) **Fatigue**
  2.) **Intergranular Stress Corrosion Cracking (IGSCC)**
  3.) **Stress Corrosion Cracking (SCC)**

- **See Figure 18-1 and 18-2**

- **BWR Vessels Bigger Than PWR**

  diameters 5.54 to 6.38 m

- **Early vessels of SA302B**
- **After 1965, used SA533B**

- **See Table 18-1**

- **Neutron exposures lower (see figure 18-8)**

- ***Lifetime exposures 5 x 10^{17} to 5 x 10^{18} n/cm^2***

- **Note effect of recent regulations**

  Figure 18-12
  Very little effect < 10^{17}

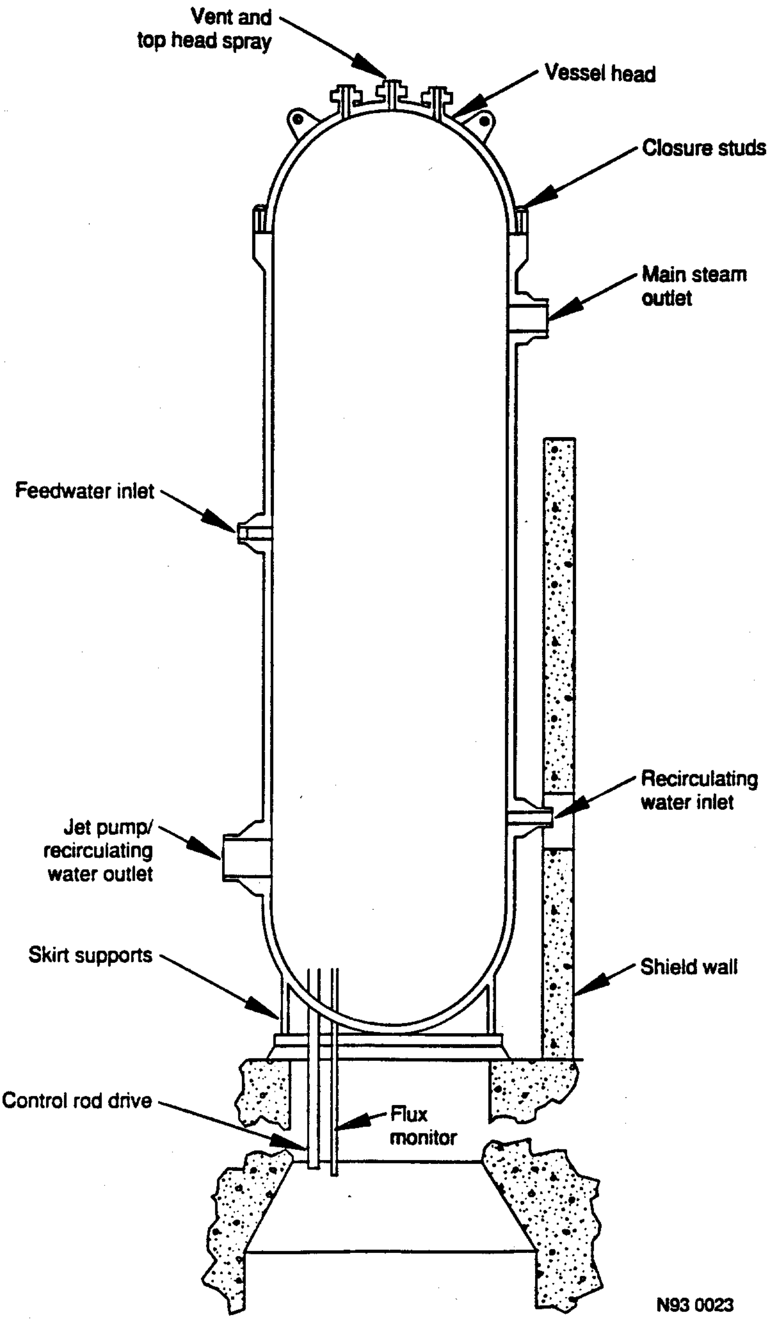

Figure 18-1. Typical BWR pressure vessel.

Table 18-1. Examples of BWR pressure vessel steels with their chemical composition.

		Average chemistry (wt%)		
Model	Material	Cu	P	Ni
BWR/3	Plate	0.17	0.10	0.58
	Weld	0.06	0.01	0.92
BWR/3	Plate	0.10	0.007	0.54
	Weld[a]	0.26	0.013	0.60
	Weld[b]	0.18	0.011	0.20
BWR/4	Plate	0.08	0.01	0.58
	Weld	0.23	0.16	<0.50
BWR/5	Plate	0.06	—	0.63
	Weld	0.07		0.71
BWR/6	Plate	0.04	—	0.59
	Weld	0.06		1.08

---

a. Submerged arch weld.

b. Electroslag weld.

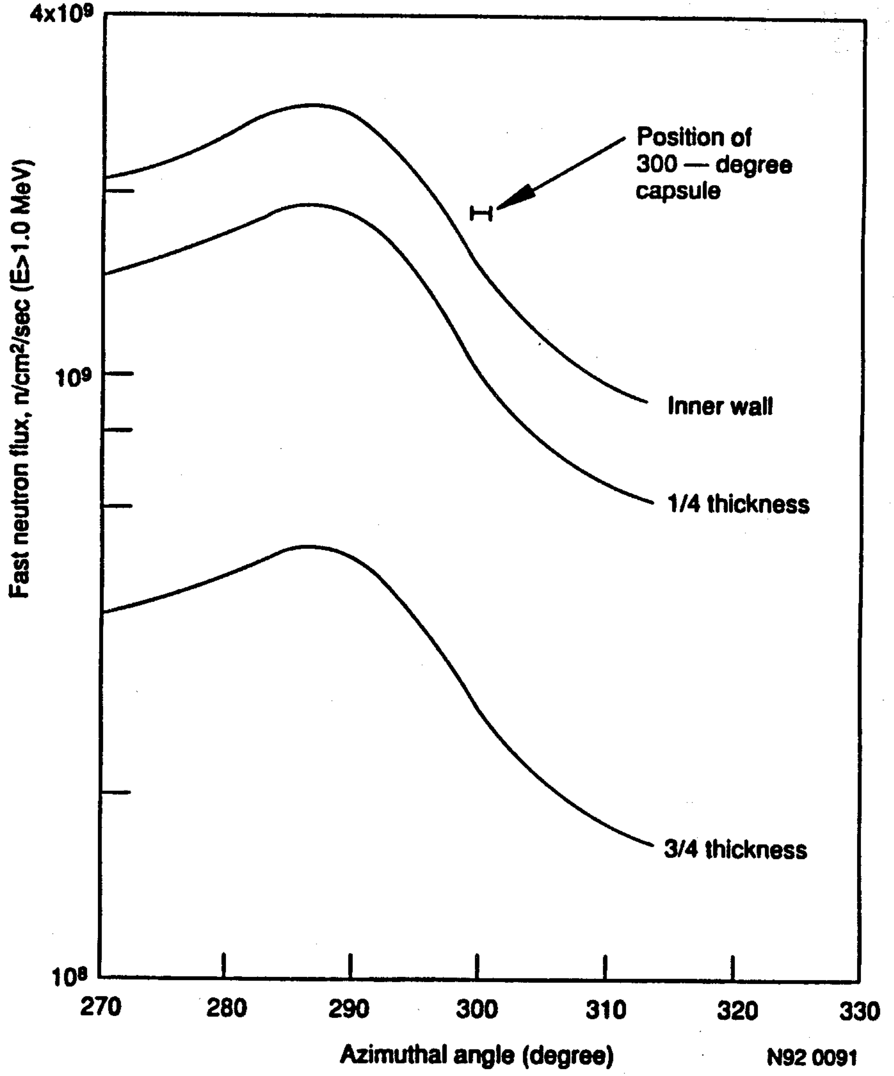

Figure 18-8. Azimuthal distribution of calculated fast neutron flux at pressure vessel inner wall, and one-fourth and three-fourths thickness (Manahan 1991).

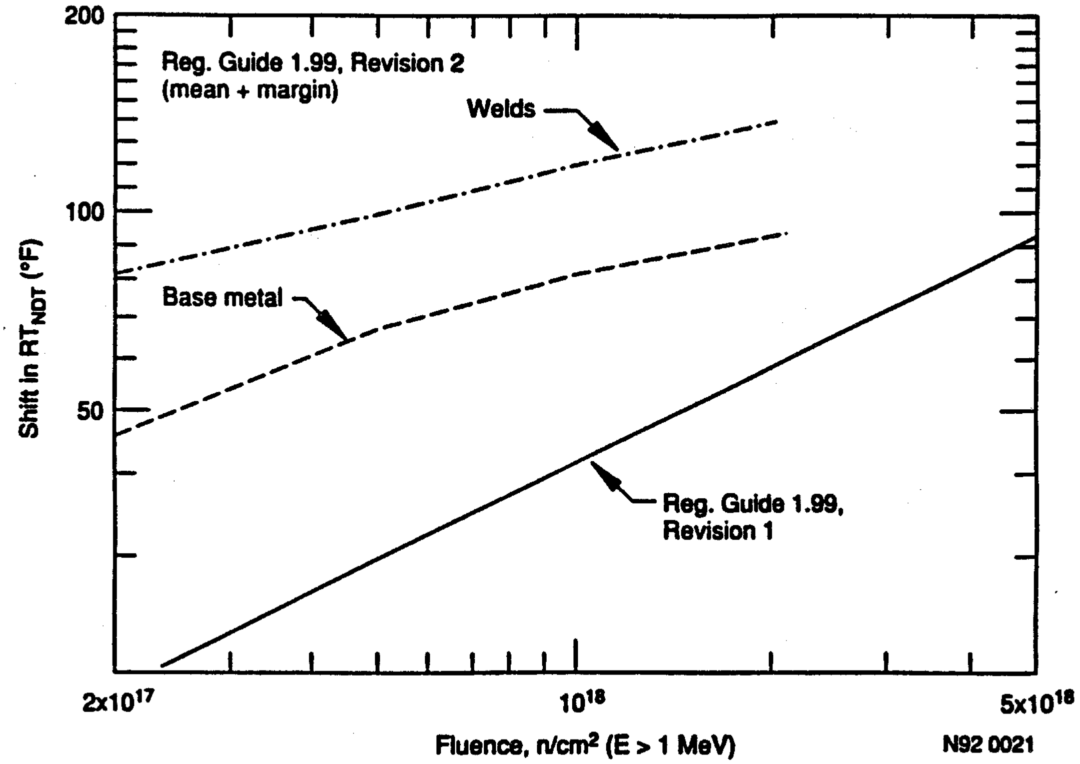

Figure 18-12. A comparison of shift predictions for welds and base metal (0.15 wt% Cu, 0.60 wt% Ni and 0.012 wt% P) calculated using Revisions 1 and 2 of Regulatory Guide 1.99.